On the anisotropic distribution of clusters in the local Universe

Schaller, M.

MNRAS 000, 1–5 (2023) Preprint 20 December 2023 Compiled using MNRAS LATEX style file v3.0

On the anisotropic distribution of clusters in the local Universe

Matthieu Schaller ★
Lorentz Institute for Theoretical Physics, Leiden University, PO Box 9506, NL-2300 RA Leiden, The Netherlands
Leiden Observatory, Leiden University, PO Box 9513, NL-2300 RA Leiden, The Netherlands

Accepted 2023 December 19. Received 2023 December 10; in original form 2023 October 09

ABSTRACT

In his 2021 lecture to the Canadian Association of Physicists Congress, P.J.E. Peebles pointed out that the brightest extra-galactic radio sources tend to be aligned with the plane of the de Vaucouleur Local Supercluster up to redshifts of $z = 0.02$ ($d_{\rm MW} \approx 85$ Mpc). He then asked whether such an alignment of clusters is anomalous in the standard ΛCDM framework. In this letter, we employ an alternative, absolute orientation agnostic, measure of the anisotropy based on the inertia tensor axis ratio of these brightest sources and use a large cosmological simulation from the Flamingo suite to measure how common such an alignment of structures is. We find that only 3.5% of randomly selected regions display an anisotropy of their clusters more extreme than the one found in the local Universe's radio data. This sets the region around the Milky Way as a 1.85σ outlier. Varying the selection parameters of the objects in the catalogue, we find that the clusters in the local Universe are never more than 2σ away from the simulations' prediction for the same selection. We thus conclude that the reported anisotropy, whilst note-worthy, is not in tension with the ΛCDM paradigm.

Key words: cosmology:large-scale structure of Universe, cosmology:theory, methods: numerical

1 INTRODUCTION

Over the last two decades, the standard cosmological model, the ΛCDM model, has received much scrutiny and passed a multitude of tests (see e.g. Dodelson & Schmidt 2020; Lahav & Liddle 2022). This vast program, designed to stress test the model and understand its limitations, will continue in this decade with exceedingly demanding precision tests, generally grouped under the Stage IV cosmology probe label. These are especially designed to help shed some light on the nature of both dark matter and dark energy as well as to explore some of the tensions currently emerging between orthogonal probes (see e.g. Abdalla et al. 2022).

One of the core tenets of our cosmology paradigm, which has arguably received comparatively less attention over the last decades, is the assumption of homogeneity and isotropy of our Universe. This Copernican assumption, coupled to Einstein's general relativity equations, allows us to fully describe the evolution and expansion of the Universe. Testing it is challenging, but, recently, tentative signs of tension have been reported in the literature (e.g. Migkas et al. 2020, 2021; Secrest et al. 2022; Kumar Aluri et al. 2023; Watkins et al. 2023). Dropping or altering this foundational assumption would, of course, have dramatic consequences on the interpretation and analysis of many other datasets and would likely require a complete redesign of our standard cosmological model.

The distribution of galaxies, clusters, or other bright sources in the local Universe is among the different tentative observational signs of anisotropy. By using the local volume as a laboratory, one can obtain clean and complete samples, which can be more challenging on larger scales. Additionally, these local probes also have the advantage of having a long history and unlike larger-scale measurements, they directly test whether *our* place in the Universe is special.

One such anomaly was reported by Peebles (2021). In his review of the ΛCDM paradigm and some of its problems, he observed that the distribution of radio sources in the local Universe ($0.01 < z < 0.02$) was not uniform on the sky. More specifically, following the exact definitions introduced later in Peebles (2022a), he noted that the 32 brightest radio sources associated with galaxies in the all-sky catalogue of van Velzen et al. (2012) and in the redshift range quoted above are found to be strongly aligned with the plane of the de Vaucouleurs Local Supercluster. As the volume surveyed contains $\sim 10^4$ galaxies, this is potentially a clear sign of alignment of massive galaxies on relatively large scales (≈ 170 Mpc). A similar signal was already reported by Shaver & Pierre (1989), also in the analysis of radio data and observations in other bands, in particular X-ray, show the same trend (Peebles 2022a). In his follow-up study, Peebles (2022b) altered slightly his selection but reached the same conclusions.

The discussion of this apparent anomaly by Peebles (2022a) then continues by asking two important questions. He, first, wondered why the clusters of galaxies appear to be near a plane at $z < 0.02$ and, secondly, whether this arrangement is unlikely within a ΛCDM framework, which he seems to suggest. He finally mention that this latter point could easily be verified by looking at large-scale structure N-body simulations.

In this letter, we directly answer this question by performing exactly the test proposed above using a catalogue of haloes extracted from a recent large ΛCDM simulation. These cover a volume large enough to contain thousands of distinct regions allowing us to estimate the

★ E-mail: mschaller@lorentz.leidenuniv.nl

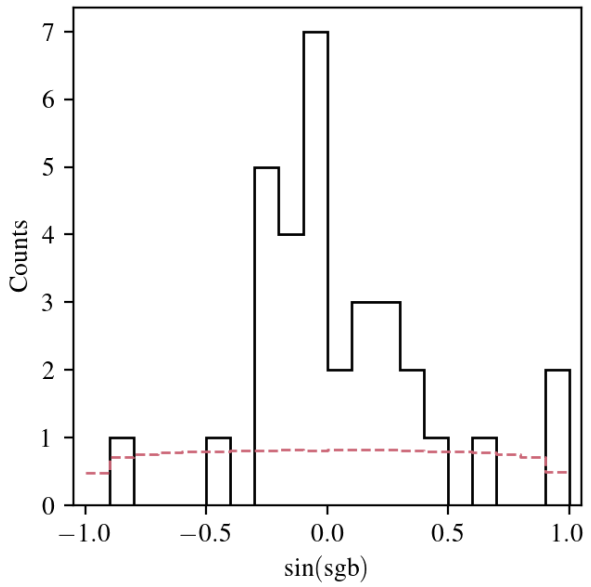

Figure 1. The 32 brightest extra-galactic radio sources from the van Velzen catalogue van Velzen et al. (2012) of radio sources in the redshift range $0.01 < z < 0.02$ binned by the sine of their super-galactic latitude (sgb). The dashed red histogram at the bottom corresponds to a uniform distribution (arbitrarily normalised) of objects with source, in the zone of avoidance (ZoA), i.e. with Galactic $|b| < 10^\circ$ removed. Our selection matches the left panel of figure 1 of Peebles (2022a). As previously reported, there is a clear anisotropy in the distribution of clusters in the local ($z < 0.02$) Universe. The anisotropy seen in the radio catalogue is not due to the presence of the ZoA.

likelihood of observing such an anisotropic distribution of bright sources in a simple frequentist way.

2 LOCAL CLUSTER ANISOTROPY

We start by reproducing the analysis of radio galaxies performed by Peebles (2022a). To be concrete, we pick one of the selections used in the literature, which we detail here for completeness. We show below that altering slightly the parameters of the selection does not change the main conclusion.

We use the van Velzen et al. (2012) radio catalogue and extract the extra-galactic sources within the redshift range $0.01 < z < 0.02$. For a fiducial cosmology with a Hubble constant $H_0 = 70$ km/s/Mpc, this corresponds to a spherical shell with inner- and outer-radii of $d_{\rm MW} \approx 45$ and ≈ 85 Mpc respectively. We then select the 32 brightest objects in this shell. The distribution of these sources in regular bins of the sine of their super-galactic latitude (sgb) is shown as the black histogram on Fig. 1. This should be compared to an isotropic distribution. However, the data suffers from potential anisotropies caused by the difficulties arising from observing through the plane of the Milky Way. Following Peebles (2022a), we thus show an isotropic distribution of sources from which a 10-degree "zone of avoidance" (ZoA) in Galactic latitude has been subtracted as the dashed red line on Fig. 1. As reported by Peebles (2022a), the 32 brightest radio sources are preferentially aligned with the super-galactic plane (sgb = 0). See also the left panel of his Fig. 1 which displays the same data, confirming that we constructed the same sample of objects. The observed anisotropy is not caused by the presence of the Galactic ZoA.

Having established the presence of an anisotropy in the local distribution of clusters, we now turn to the construction of a quantitative metric of the anisotropy.

To characterize the anisotropy in absolute terms, *i.e.* without reference to a particular direction, we borrow the tools used for the analysis of planes of satellites around the Milky-Way (e.g. Pawlowski et al. 2015; Sawala et al. 2023) and base our analysis around the reduced inertia tensor generated by the distribution of sources:

$$I_{ij} = \sum_{n=1}^{N} \mathbf{x}_{n,i}\mathbf{x}_{n,j}, \tag{1}$$

where $\mathbf{x}_n$ are the coordinates of the n-th cluster with respect to the observer after projection onto a unit sphere. We choose to use the reduced tensor so as to not be affected by distant outliers; this definition is also close to the idea of angle on the sky used in the original Peebles (2022a) analysis. We label the square roots of the tensor's eigenvalues (*i.e.* the three axis of the ellipsoid of inertia) as a, b and c (in decreasing size) and define the anisotropy as the ratio c/a. A perfectly isotropic distribution of points would display a c/a ratio of one whilst a perfectly planar distribution would have $c/a = 0$.

Applying this procedure to the 32 brightest sources selected by Peebles (2022a) from the van Velzen et al. (2012) radio catalogue in the distance range $0.01 < z < 0.02$, we find an anisotropy $c/a_{\rm data} = 0.464$. For completeness, we also computed the intermediate-to-major axis ratio $b/a_{\rm data} = 0.713$. This indicates that the distribution of radio sources is an oblate, flattened distribution.

3 SIMULATIONS

The simulation used for our analysis is taken from the Virgo Consortium's FLAMINGO[1] suite (Schaye et al. 2023; Kugel et al. 2023). These simulations, performed using the SWIFT cosmology code (Schaller et al. 2023), assume a standard flat ΛCDM cosmology with Gaussian initial conditions and parameters $h = 0.681, \Omega_{\rm m} = 0.306, \Omega_\Lambda = 0.694, n_s = 0.967, \sigma_8 = 0.807$, which corresponds to best-fit ΛCDM model to the Dark Energy Survey year three data combined with external constraints (the model labelled "3×2pt + All Ext." of Abbott et al. (2022)). More specifically, we make use of the main "dark matter only" simulated volume (`L2p8_m9_DMO`) which evolves 5040^3 cold dark matter particles in a volume of 2.8^3 Gpc^3. This combination leads to a particle mass of $6.72 \times 10^9 {\rm M}_\odot$, sufficient to fully resolve haloes with a mass of $10^{12} {\rm M}_\odot$, *i.e.* more an order of magnitude lower than the haloes in which the sources discussed in the previous section are expected to reside. Note that for the purpose of identifying the alignment of large structures on scales of 10s of Mega-parsec, a simulation evolving only dark matter is sufficient as baryonic and astrophysics processes won't affect structures on these scales (Schaye et al. 2023). We use the redshift zero output of the simulation and identify haloes and their centres in the snapshot using the phase-space structure finder VELOCIRAPTOR (Elahi et al. 2019).

4 RESULTS AND ANALYSIS

We now perform an analysis of the simulations to obtain the frequency of systems as anisotropic as the ones observed in the local Universe.

[1] https://flamingo.strw.leidenuniv.nl/

4.1 Direct comparison

To mimic the source catalogues introduced above, we place $N = 5000$ observers randomly in the simulation volume[2]. Note that we do not explicitly select observers to lie on a specific matter sheet, as is the case of the MW which resides on the sheet of the local Supercluster. We are thus asking what the anisotropies would look like for a truly random observer rather than for the ones embedded in a local structure. By design, this choice increases the chance that our local environment is anomalous and is hence a good basis for a null-test.

For each observer, we construct an all-sky shell and include all objects at a distance 45 Mpc $<$ r $<$ 85 Mpc of the observer. To mock the zone of avoidance created by the plane of the Milky Way disk, we draw a random vector for each of these observers and define the observer's galactic disk as the plane perpendicular to this vector. The key underlying assumption here being that the orientation of the plane of the MW disk is in no way related to any large-scale plane of clusters or filaments. We then eliminate from our source catalogues all the objects within 10° of this plane. Finally, we select the centres of the 32 largest haloes in each of the regions as a proxy for the selection of the 32 brightest radio sources. From their location, we construct the reduced inertia tensor (eq. 1) of each of these mock catalogues and compute their anisotropies c/a.

The distribution of anisotropies is shown in Fig. 2. The distribution of anisotropies is exceptionally well fit by a Gaussian with a mean c/a of 0.637 and a standard deviation of 0.094 [3]. The vertical dashed line indicates the anisotropy measured for the local catalogue of radio sources. 96.5% of all random mock observers see a distribution on the sky of their brightest 32 objects within 45 Mpc $<$ r $<$ 85 Mpc that is more isotropic than the one we obtained in the local Universe. At face value, this puts the region around the MW as a 1.85σ outlier towards more anisotropic distributions.

For completeness, we also measured the intermediate-to-major axis ratio (b/a) using the same inertia tensor for all our virtual observers. We find a distribution of b/a axis ratios with mean 0.812 and standard deviation 0.087, indicating that, similarly to the local Universe data, the virtual observers see oblate distribution of sources.

As Pawlowski et al. (2015) pointed out, valuable information can be lost when considering only the reduced inertia tensor and not the full tensor. We have repeated the analysis of both the data and simulation using the full inertia tensor and have obtained virtually indistinguishable results ($c/a_{\rm data} = 0.467$ and a Gaussian distribution in the simulation characterized by a mean $c/a = 0.631$ and a standard deviation of 0.095). We interpret this minimal difference as being the natural consequence of the narrow range of distances considered in the original selection of radio sources by Peebles (2022a).

4.2 Properties of the objects probed

As we started from a catalogue of bright radio sources which we compare to a simulation without baryonic physics, it is interesting to check whether the haloes we used are sensible hosts of radio galaxies. For each of the 5000 random observers, we recorded the least and most massive objects they encountered in the radial shells they used for the anisotropy calculations. For all observers, we find that the largest of the 32 objects included in the selection lies in the range $M_{200} = 1.0 \times 10^{14}$ M$_\odot$ $- 5 \times 10^{15}$ M$_\odot$. Similarly, the *smallest* object they encountered lies in the range $M_{200} = 3.5 \times 10^{13}$ M$_\odot$ $- 1.5 \times 10^{14}$ M$_\odot$. At the resolution of our simulation, these are all extremely well resolved haloes. They are also the hosts of large groups of galaxies or even large clusters. We expect such haloes to all host large central galaxies which will be radio bright (see e.g. Mandelbaum et al. 2009) and would clearly be part of the selection made by van Velzen et al. (2012) had they been observing these regions of the simulation.

As an additional cross-check, the range of halo masses quoted above is also in agreement with the estimates of masses made for the objects in the local Universe (see e.g. Stopyra et al. 2021).

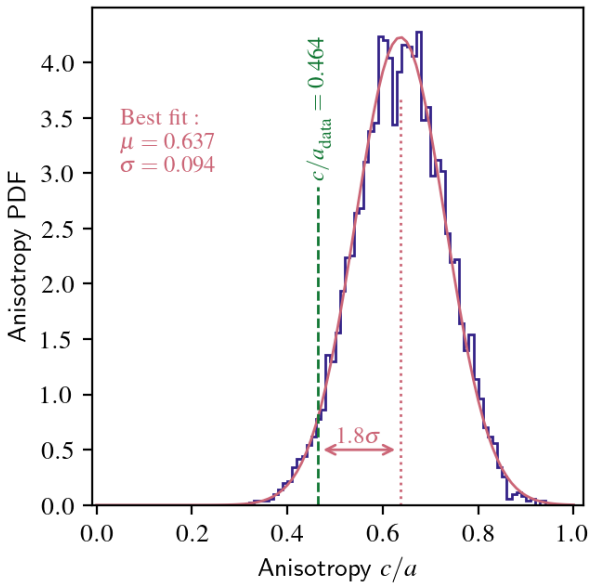

Figure 2. Distribution of the anisotropy of the 32 most-massive clusters in 5000 randomly selected regions of size 45 Mpc $< r <$ 85 Mpc extracted from the FLAMINGO simulation volume (blue histogram). The solid red line is a Gaussian fit to the distribution whose mean is indicated by the vertical dotted line and parameters are given in the figure. The green vertical dashed line indicates the anisotropy of the sample of 32 radio sources of Fig. 1. The observed anisotropy in the data is a 1.85σ outlier towards more anisotropic systems.

4.3 Varying the parameters of the problem

The analysis presented above relies on a specific choice for the radial range used and for the number of objects to retain when computing the angular distribution or anisotropy. To strengthen our conclusions, we repeat, here, the analysis by varying these aforementioned parameters.

We start by keeping the radial range fixed but changing the number of objects to consider. Instead of choosing the 32 brightest sources in the radio catalogue, we let this number float. For each selection, we compute the corresponding inertia tensor and reduced anisotropy. This latter value is reported as a function of the number of sources on the top panel of Fig. 3. We then return to the simulation and for each of the 5000 random observers, we compute the anisotropy based on the top N largest haloes in the radial range 45 Mpc $< r <$ 85 Mpc after removal of a mock zone of avoidance (see above). The fraction of observers with an anisotropy of their clusters more pronounced than the data is reported in the middle panel of Fig. 3. Finally, for each choice of N, we compute the mean and standard deviation of

[2] Using close-packing there are ≈ 5800 independent spheres in our simulation volume. We use 5000 observers to avoid repetitions.

[3] A K-S test between the bins and the fit returns a p-value of $< 10^{-6}$.

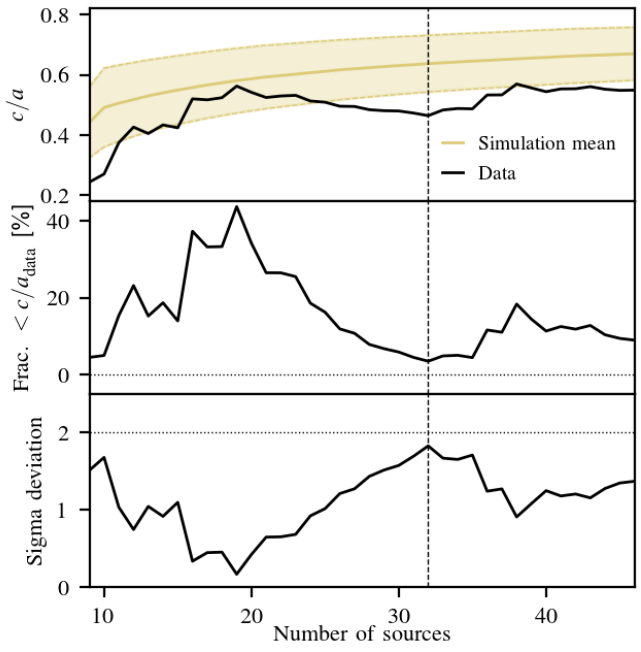

Figure 3. A repeat of the analysis for varying number of sources in the catalogue. *(top)* The anisotropy of the top N brightest sources in the van Velzen catalogue in the radial range 45 Mpc < r < 85 Mpc (black) and the mean and standard deviation of the distribution obtained from 5000 random observers in the simulation (yellow). *(middle)* The fraction of regions of the same size in the simulation that have a flatter distribution of their top N most massive clusters. *(bottom)* The deviation from the simulation's mean of the observed c/a in units of the standard deviation of the distribution. On all panels, the dashed line indicates the number of sources chosen by Peebles (2022a) and corresponds to the results shown in Fig. 2. For no choice of the number of sources does the observed local anisotropy deviates at the 2σ level or more from the simulation-inferred ΛCDM expectation.

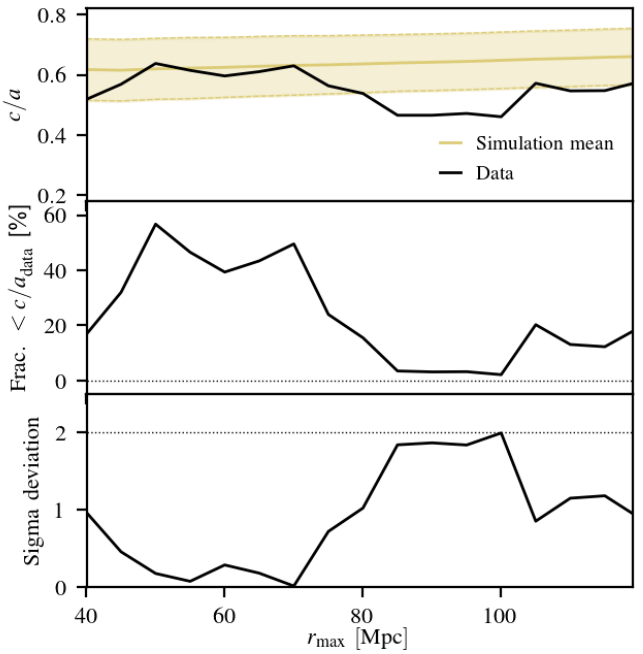

Figure 4. Same as Fig. 3 but varying the radial range used to select the clusters. *(top)* The anisotropy of the top 32 brightest sources in the van Velzen catalogue in the radial range between a minimum of 30 Mpc and a maximum given on the x-axis (black) and the mean and standard deviation of the same measurement across 5000 random observers in the simulation (yellow). *(middle)* The fraction of regions of the same size in the simulation that have a flatter distribution of their top 32 most massive clusters. *(bottom)* The deviation from the simulation's mean of the observed c/a in units of the standard deviation of the distribution. For no radial range choice does the observed local anisotropy deviates at the 2σ level or more from the simulation-inferred ΛCDM expectation.

c/a and report the distance from the mean of the observed one in units of the standard deviation on the bottom panel of Fig. 3.

We find that for all values of N, the deviation from the ΛCDM expectation, given by the simulation, of the observed anisotropy of local clusters never reaches a 2σ threshold.

The other variable in the problem is the choice of radial range away from the Milky Way where the radio sources (or clusters) are selected. We explore this now by varying the thickness of the radial shell from which the clusters are selected. We keep the inner radius fixed and vary the maximum one. In order to always have enough sources, we reduce the inner radius to $r_{\rm min} = 30$ Mpc. For each shell thickness, we select the 32 brightest sources in the catalogue or the 32 most massive haloes in the simulation. The result of the experiment as a function of the shell outer-radius $r_{\rm max}$ is displayed in Fig. 4. As was the case when varying the number of sources, we find that the anisotropy found in the data never reaches a 2σ deviation from the simulation's mean.

It is interesting to notice that the data is found to be most anisotropic when compared to the simulation's mean when taking a shell reaching up to $r_{\rm max} = 80 - 100$ Mpc. This is the distance at which the Perseus supercluster is located.

5 CONCLUSION

In this letter, we directly answer the question asked by Peebles (2021) where he wondered whether the observed distribution of massive clusters in the very local Universe ($z < 0.02$) is in tension with the standard cosmological model.

To achieve this, we used one of the large ΛCDM N-body simulations of the Flamingo suite (Schaye et al. 2023) to study the isotropy of the distribution of clusters in spheres of radius ≈ 70 Mpc. More specifically, we made mimicked the selection of bright radio sources, done by Peebles (2022a), that revealed the anisotropic distribution of clusters in the Local Universe. By placing 5000 random observers in the simulation, each constructing the same mock survey, we were able to construct the anisotropy of clusters in shells of 45 Mpc < r < 85 Mpc for a ΛCDM cosmology with Gaussian initial conditions. We then used the reduced inertia tensor, constructed from the clusters' centres, and its eigenvalues as a measure of the isotropy of the clusters in each region and found that the anisotropy identified in the Local Universe data (Fig. 1) is a 1.85σ outlier (Fig. 2) from the ΛCDM-based prediction. In other words, 96.5% of the regions in the simulation display an arrangement of their 32 most massive clusters in the aforementioned radial shell that is more isotropic than what the radio data of van Velzen et al. (2012) reveals.

We then varied the parameters of the selection by changing the number of objects selected (Fig. 3) and the radial range (Fig. 4). In both cases, we found that the observational data never reaches a 2σ

threshold compared to the simulation-inferred ΛCDM-prediction.

We thus conclude that the anisotropy in the distribution of bright sources revealed by Peebles (2021, 2022a,b) in the all-sky radio data of van Velzen et al. (2012) and Shaver & Pierre (1989) (as well as in survey data using other wavelengths) is not a problem for the ΛCDM model.

ACKNOWLEDGMENTS

We thank Carlos Frenk, Jim Peebles, and Till Sawala for useful comments on an early draft of this manuscript as well as the Flamingo collaboration for making their simulation data available.
This work used the DiRAC@Durham facility managed by the Institute for Computational Cosmology on behalf of the STFC DiRAC HPC Facility (www.dirac.ac.uk). The equipment was funded by BEIS capital funding via STFC capital grants ST/K00042X/1, ST/P002293/1, ST/R002371/1 and ST/S002502/1, Durham University and STFC operations grant ST/R000832/1. DiRAC is part of the National e-Infrastructure.

DATA AVAILABILITY

The data from the Flamingo suite will be made public once practically feasible given the challenging size of the datasets. In the mean time, the data can be accessed upon requests to the authors.

REFERENCES

Abbott T. M. C., et al., 2022, Phys. Rev. D, 105, 023520
Abdalla E., et al., 2022, Journal of High Energy Astrophysics, 34, 49
Dodelson S., Schmidt F., 2020, Modern Cosmology. Academic press, doi:10.1016/C2017-0-01943-2
Elahi P. J., Cañas R., Poulton R. J. J., Tobar R. J., Willis J. S., Lagos C. d. P., Power C., Robotham A. S. G., 2019, Publ. Astron. Soc. Australia, 36, e021
Kugel R., et al., 2023, MNRAS, 526, 6103
Kumar Aluri P., et al., 2023, Classical and Quantum Gravity, 40, 094001
Lahav O., Liddle A. R., 2022, arXiv e-prints, p. arXiv:2201.08666
Mandelbaum R., Li C., Kauffmann G., White S. D. M., 2009, MNRAS, 393, 377
Migkas K., Schellenberger G., Reiprich T. H., Pacaud F., Ramos-Ceja M. E., Lovisari L., 2020, A&A, 636, A15
Migkas K., Pacaud F., Schellenberger G., Erler J., Nguyen-Dang N. T., Reiprich T. H., Ramos-Ceja M. E., Lovisari L., 2021, A&A, 649, A151
Pawlowski M. S., Famaey B., Merritt D., Kroupa P., 2015, ApJ, 815, 19
Peebles P. J. E., 2021, arXiv e-prints, p. arXiv:2106.02672
Peebles P. J. E., 2022a, Annals of Physics, 447, 169159
Peebles P. J. E., 2022b, MNRAS, 511, 5093
Sawala T., et al., 2023, Nature Astronomy, 7, 481
Schaller M., et al., 2023, arXiv e-prints, p. arXiv:2305.13380
Schaye J., et al., 2023, MNRAS, 526, 4978
Secrest N. J., von Hausegger S., Rameez M., Mohayaee R., Sarkar S., 2022, ApJ, 937, L31
Shaver P. A., Pierre M., 1989, A&A, 220, 35
Stopyra S., Peiris H. V., Pontzen A., Jasche J., Natarajan P., 2021, MNRAS, 507, 5425
van Velzen S., Falcke H., Schellart P., Nierstenhöfer N., Kampert K.-H., 2012, A&A, 544, A18
Watkins R., et al., 2023, MNRAS, 524, 1885